ISSN 1674-1056
http://cpb.iphy.ac.cn
http://iopscience.iop.org/cpb
中国物理 B
Chinese Physics
中国物理
Chinese Physics B

Tunable edge bands and optical properties in black phosphorus nanoribbons under electric field

Hong Liu(刘红)

Citation: Chin. Phys. B . 2018, 27(12): 127301. **doi:** 10.1088/1674-1056/27/12/127301

What follows is a list of articles you may be interested in

Distinct edge states and optical conductivities in the zigzag and armchair silicene nanoribbons under exchange and electric fields

Jianfei Zou(邹剑飞), Jing Kang(康静)

Chin. Phys. B . 2018, 27(3): 037301. **doi:** 10.1088/1674-1056/27/3/037301

Highly stable two-dimensional graphene oxide: Electronic properties of its periodic structure and optical properties of its nanostructures

Qin Zhang(张琴), Hong Zhang(张红), Xin-Lu Cheng(程新路)

Chin. Phys. B . 2018, 27(2): 027301. **doi:** 10.1088/1674-1056/27/2/027301

Modulating the properties of monolayer C_2N: A promising metal-free photocatalyst for water splitting

Song Yu(俞松), Yong-Chao Rao(饶勇超), Xiang-Mei Duan(段香梅)

Chin. Phys. B . 2017, 26(8): 087301. **doi:** 10.1088/1674-1056/26/8/087301

Band structure of silicon and germanium thin films based on first principles

Xue-Ke Wu(吴学科), Wei-Qi Huang(黄伟其), Zhong-Mei Huang(黄忠梅), Chao-Jian Qin(秦朝建), Tai-Ge Dong(董泰阁), Gang Wang(王刚), Yan-Lin Tang(唐延林)

Chin. Phys. B . 2017, 26(3): 037302. **doi:** 10.1088/1674-1056/26/3/037302

Effect of size and indium-composition on linear and nonlinear optical absorption of InGaN/GaN lens-shaped quantum dot

Ahmed S Jbara, Zulkafli Othaman, M A Saeed

Chin. Phys. B . 2016, 25(5): 057801. **doi:** 10.1088/1674-1056/25/5/057801

SPECIAL TOPIC — 60th Anniversary of Department of Physics of Nanjing Normal University

Tunable edge bands and optical properties in black phosphorus nanoribbons under electric field*

Hong Liu(刘红)†

Physics Department, Nanjing Normal University, Nanjing 210023, *China*

(Received 3 August 2018; revised manuscript received 4 November 2018; published online 25 November 2018)

For several types of the applied electric field configuration on the normal-zigzag black phosphorus nanoribbon (nZZ-BPNR) we investigate the band structure and the linear optical absorption spectrum, especially for the edge states and the corresponding low-energy absorption peaks. The obtained results show that the applied electric field can not only open another band gap at $k = 0.5$ point, but also can change completely the spacial probabilities of edge states in the two edge bands. The strength of electric field can tune the two band gaps at the Γ point and 0.5 point. Further, one remarkable feature is that the forbidden transition E_{12} and E_{21} are allowed. The lowest-excited-energy linear absorption peak E_{11} originates from the transition between two edge bands at the Γ point. Finally, in comparison with the lowest-excited-energy peaks among various configurations, the second type of electric field configuration can move this peak blue-shift larger than other configurations.

Keywords: black phosphorus nanoribbon, edge band, linear optical absorption spectrum

PACS: 73.20.At, 78.90.+t **DOI:** 10.1088/1674-1056/27/12/127301

1. Introduction

Two-dimensional black phosphorus (BP) provide enormous potential in electronic and optoelectronic applications due to the tunable and moderate direct band gap and the high carrier mobility. Significant efforts have been devoted to investigate its electronic, optical, and mechanical properties,[1–7] which is the foundation for next-generation chip-scale integrated devices. With respect to the optical properties, BP-based photo-device's shape and size affect device performance due to the spacial confinement effect.[2–4,8,9] Some related reviews on photonics and fabrication of BP can be read in Refs. [1], [5], [6], and [7]. Zhang *et al.* proposed and confirmed experimentally that the band-gap and optical properties can be tuned by doping with metal–ion onto the surface of BP.[10] In recent months the optical properties of few-layer black arsenic phosphorus can be tuned by the electric field.[11] In last year the theoretical work on investigating the electric- and magnetic-field dependence of the electronic and optical properties of phosphorene quantum dots has been done.[12] Remarkably, in these days two groups applied the top gate voltage and bottom gate voltage on monolayer topological WTe_2 to realize the electrically tunable low-density superconductivity.[13,14] Therefore, it excites more and more interesting study on the electric tune of electtic structure and optical properties of various two-dimensional topological materials.

Via first-principles simulations the optical absorption spectra and excitons of monolayer black phosphorus (phosphorene) nanoribbons (BPNRs) has been theoretically studied.[15,16] Unfortunally, at the edge atoms of BPNRs they adhere to hydrogen atoms in order to obtain the stable geometrical structure. The adhering hygrogen atom leads to the opening of band gap, however, there are not the edge bands in the band structure.

Based on the tight-binding (TB) model, remarkably, in the normal-zigzag black phosphorus nanoribbon (nZZ-BPNR) a prominent feature is the presence of a quasi-flat edge band entirely detached from the bulk band,[3,4,12,17–23] which is different from the zero-energy edge bands in zigzag grapheme nanoribbon (ZGNR).[24–28] The exciton structure of black phosphorus quantum dots[4] and exciton Stark shift in BP[29] have been theoretically investigated. They adopted the 10 hopping parameter TB model.[2] Pederson *et al.* have devote hard theoretical work to investigate the nonlinear optical response of monolayer phosphorene,[30] and the optical third harmonic generation of BP on the base of the tight binding model, in which the hopping and overlap integrals are evaluated with density functional tight binding.[31]

The in-plane applied electric field along the ribbon width can tune the band structure and optical properties of black phosphorus nanoribbon (BPNR).[17,22] Due to two atom sublayers along the z axis in nZZ-BPNR, one can apply the different electric fields on the upper (lower) sublayer.[11,12,23] In this paper, the lattice structure of nZZ-BPNR shows in Fig. 1. Based on the former research work, we propose several types of the applied electric field configuration on nZZ-BPNR to

*Project supported by the National Natural Science Foundation of China (Grant No. 10947004) and the Jiangsu Government Scholarship for Overseas Studies.

†Corresponding author. E-mail: liuhong3@njnu.edu.cn

© 2018 Chinese Physical Society and IOP Publishing Ltd

study the band structure and the linear optical absorption spectrum, especially for the edge states and the corresponding low-energy absorption peaks. The nZZ-BPNR absorption gap with low-energy absorption peaks can be tunable by the electric field. Comparison of band structure and optical absorption characteristics under different types of electric fields we hope these research results to be helpful for the future design of optoelectronic nano devices. We hope that these two recent experiment skills[13,14] can help one to reproduce our theoretical work in the future.

In what follows, we introduce structures and provide theoretical details of calculations in Section 2, discuss the results in Section 3, and summarize the discussion in Section 4.

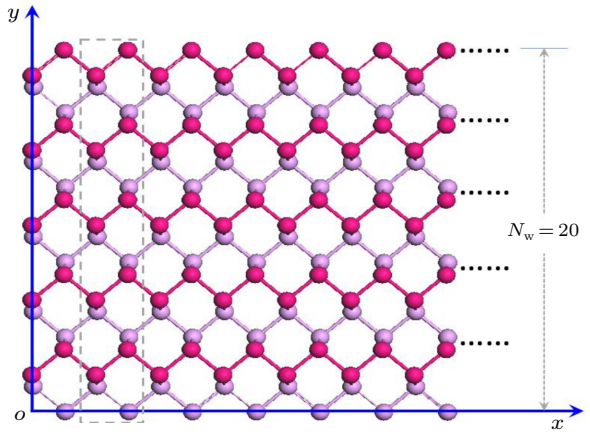


Fig. 1. (color online) The geometrical structure of nZZ-BPNR with the width $N_w = 20$ (the number of atoms in one unit cell). The unit cell is shown in the dashed rectangle frame.

2. Theoretical model

We employ the tight-binding Hamiltonian derived recently by Rudenko *et al.* for phosphorene[2]

$$\hat{H} = \sum_{i \neq j} t_{ij} c_i^{\dagger} c_j + \sum_{i \in \alpha} V_{\alpha} c_i^{\dagger} c_i, \tag{1}$$

where $c_i^{\dagger}$ (c_i) is the electron creation (annihilation) operators at site i, and t_{ij} are parameters describing the hopping energy between the lattice sites i and j up to the tenth nearest neighbor site, while V_{α} (α = A, B or C) is the electrical potential energy induced by the different applied gate voltages on three different regions A, B, and C shown in Fig. 4. The basis set of wave function is $\{\phi_i(\boldsymbol{k})\}$ $(i = 1, 2, 3, \ldots, N_{\text{cell}})$, in which $\phi_i(\boldsymbol{k})$ is the Fourier transform of the atomic orbital function $\varphi_i(\boldsymbol{r})$ at site i. So the solved wave function of system for the n-th eigenenergy $E_n(\boldsymbol{k})$ at $\boldsymbol{k}$ point is written as

$$\psi_n(\boldsymbol{k}) = \left(c_1^n(\boldsymbol{k}), c_2^n(\boldsymbol{k}), c_3^n(\boldsymbol{k}), \ldots, c_{N_{\text{cell}}}^n(\boldsymbol{k})\right). \tag{2}$$

The spacial probability of the wave function $\psi_n(\boldsymbol{k})$ is $\rho_i^n(\boldsymbol{k}) = c_i^{n\dagger}(\boldsymbol{k}) c_i^n(\boldsymbol{k})$ at the site i.

The analytic expression of the linear optical absorption spectrum takes the general form[32–37]

$$\alpha(\omega) \approx \omega \sum_{\boldsymbol{k}} \left| \boldsymbol{e}_E \cdot (\boldsymbol{M}_{\boldsymbol{k}}^{cv})^* \right|^2 \frac{\gamma}{(\hbar\omega - E_{\boldsymbol{k}}^{cv})^2 + \gamma^2}, \tag{3}$$

where the transition energy $E_{\boldsymbol{k}}^{cv} = E_{\boldsymbol{k}}^c - E_{\boldsymbol{k}}^v$ of each band-to-band contribution. The unit of wave vector (k_x, k_y) is ($2\pi/a$, $2\pi/b$), in which the lattice constants $a = 3.314$ Å (zigzag), $b = 4.376$ Å (armchair).[39,40] The $\boldsymbol{e}_E$ denotes the polarization direction of the incident laser. Lorentzian homogeneous broadening is included with $\gamma = 0.01$ eV. The interband dipole matrix is written as[34,35,40]

$$\boldsymbol{M}^{cv}(\boldsymbol{k}) = \frac{-e\left\langle \psi_{\boldsymbol{k}}^c | \hat{H}\boldsymbol{r} - \boldsymbol{r}\hat{H} | \psi_{\boldsymbol{k}}^v \right\rangle}{E_{\boldsymbol{k}}^c - E_{\boldsymbol{k}}^v}, \tag{4}$$

where $\hat{H}$ is the Hamiltonian of the system, and $\psi_{\boldsymbol{k}}^c$ ($\psi_{\boldsymbol{k}}^v$) and $E_{\boldsymbol{k}}^c$ ($E_{\boldsymbol{k}}^v$) are the wave functions and the energies of the conduction band (c) (valence band (v)) at a given k-vector for the transition $v \to c$, respectively. In this work, we only consider direct transitions among bands. Firstly, according to the obtained band structure in Fig. 2(a) based on the Hamiltonian in Eq. (1), involving all transitions between two conduction bands and two valence bands. Through the Brillouin zone integration we calculate the linear absorption spectrum for two-dimensional monolayer phosphorene shown in Fig. 2(b).

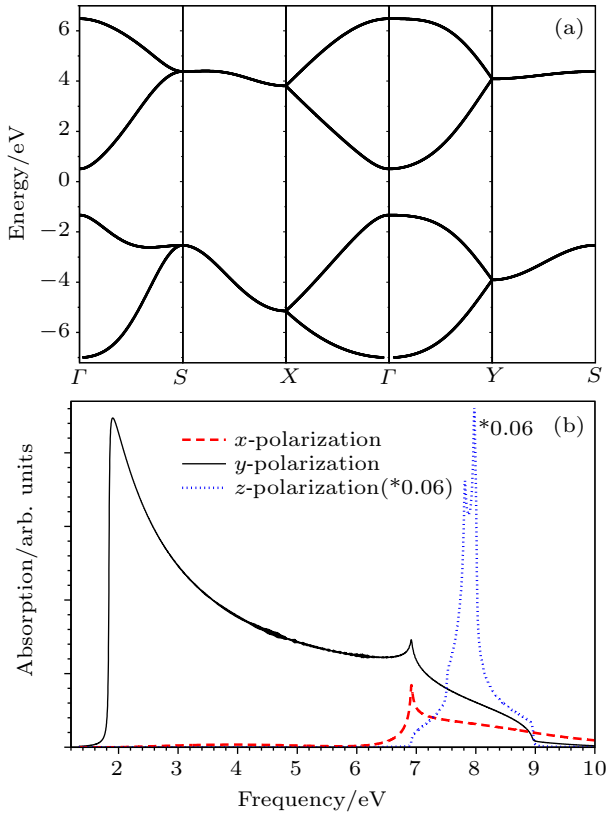


Fig. 2. (color online) The band structure (a) and the linear absorption spectrum (b) of monolayer phosphorene. For panel (b) the total numer of k-point is $N_x \cdot N_y = 8 \times 10^4$ large enough to make the curve lines smooth in the calculation.

Obviously, there is an extraordinarily large optical anisotropy. In the low-energy region the y-polarized absorption is the strongest, in the narrow high-energy region 7.0 eV $\sim$ 9.0 eV the absorption peak for the z-polarized incident laser is 16 times stronger than the peak of y-polarized absorption at 1.8 eV, which is the same to the optical conductivity σ_{xx}.[2]

For the nZZ-BPNR shows in Fig. 1, not considering the applied electric field, with different widths, we calculated the band structure shown in Fig. 3(a). When the width is narrow, there two edge bands. With the increase of width the two edge bands are close to each other, which is in agreement with the results in the work.[22,23] Obviously, the two edge bands are the quasi-flat edge bands near the Fermi energy that is entirely detached from the bulk bands. For large width nZZ-BPNR this quasi-flat edge band is two-fold degenerate not considering spin degree. According to the spacial occupied probability of these states in two edge bands in Figs. 5(a1)–5(a2), at $k = 0.5$ the electron of edge state does not localize at one edge site, but at two opposite edge sites 50%, respectively. This character is different from the edge states in zigzag graphene nanoribbon.[42,43]

Based on the band structure obtained above, with the increase of width the low-energy-excited linear absorption spectrum for the left-circle incident laser is shown in Fig. 3(b).

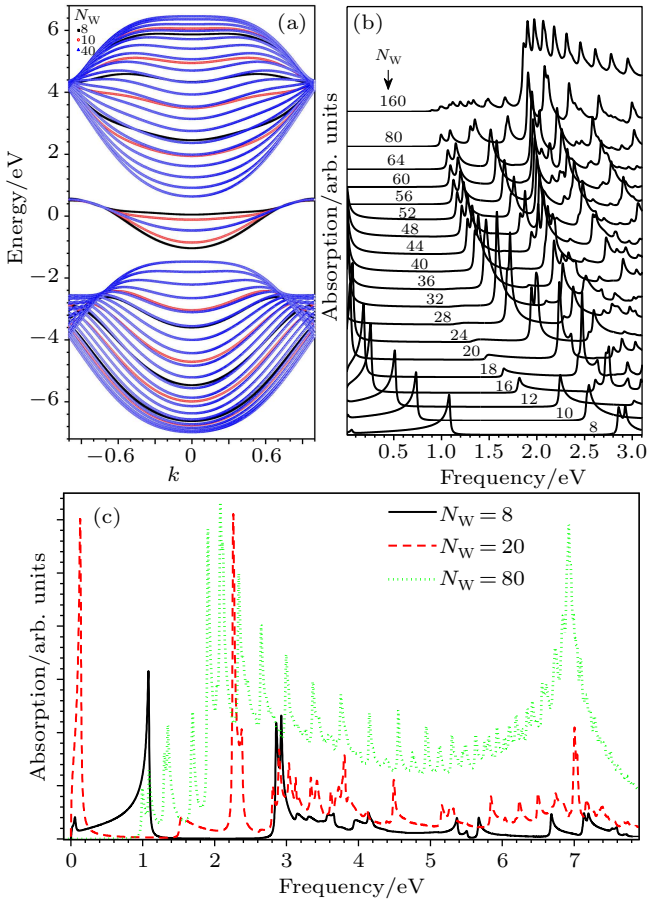


Fig. 3. (color online) The band structures (a) and the y-polarized linear absorption spectra [(b)–(c)]. The integers denote the widths of nZZ-BPNRs.

Compared with that in Fig. 2(b), there are some low-energy-excited peaks below 2.0 eV. The size effect and the position of low-energy-excited peaks are in agreement with the theoretical work.[12] With the increase of width the number of low-energy-excited peaks increases, but the peak intensity decreases. When $N_w < 32$, there is several much stronger low-energy peaks than the high-energy peaks. For the narrow width BPNR ($N_w < 52$) the lowest-energy-excited peak from the excitation between two edge bands is close to zero from 1.0 eV (when $N_w = 8$) in Fig. 3(c). The low-excited energy is the energy region of interest for nZZ-BPNR. Therefore, in this paper we take the narrow nZZ-BPNR ($N_w = 20$) as an example to study the effect of electric field on band structure and linear optical properties.

According to the geometrical structure of nZZ-BPNR there are four divided space regions to apply the electric field denoted by different colors in Fig. 4. Considering the situation in practical application, it should be existence of the middle region without the action of applied electrical field denoted by gray color ($V_G = 0$), which is to avoid the contact between two neighbor regions under different electric voltages. Therefore, we can design five types of the applied electric field configurations to study the electronic and optical properties of nZZ-BPNR in order to investigate the way to tune the band structure, specially the edge bands. Firstly, according to z coordinate we apply two different electrical potentials on two atom sublayers: $V_{GA} = \xi$ ($z > 0$) and $V_{GB} = -\xi$ ($z < 0$) shown in

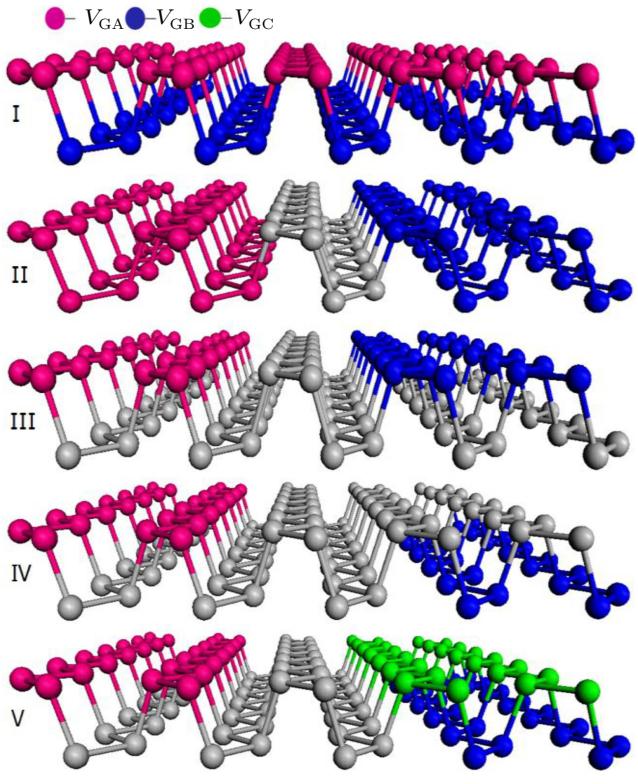


Fig. 4. (color online) The schematic diagrams of five types of electric field configuration on the two or three regions A, B, and C denoted by red, blue, and green color, respectively, in nZZ-BPNR ($N_w = 20$).

Fig. 4(I). The second type II is to divide cell into two regions having two different electrical potentials according to y coordinate: A ($y < y_9$) and B ($y > y_{12}$), where $y_{9(12)}$ is the y coordinate of site 9(12). The third type III is to divide the up-sublayer into two regions according to y coordinates: A and B. The fourth type IV is the A ($z > 0$, $y < y_9$), B ($z < 0$, $y > y_{12}$). Based on the fourth type, we add the region C ($z > 0$, $y > y_{12}$) in the type V.

3. Band structure and optical properties under applied electronic field

For the former four types of electric field distribution configurations in Fig. 4 we apply two different electric potentials on two different regions: $V_{GA} = \xi$ and $V_{GB} = -\xi (0 \leq \xi \leq 0.50$ eV). Wondrously, even if applying very weak electric potential the most remarkable change in band structure is that the spacial probability of edge states at $k = 0.5$ becomes 100% at one single edge site shown in Figs. 5(b1) and 5(b2), which is similar to the edge states in ZGNRs.[41–43]

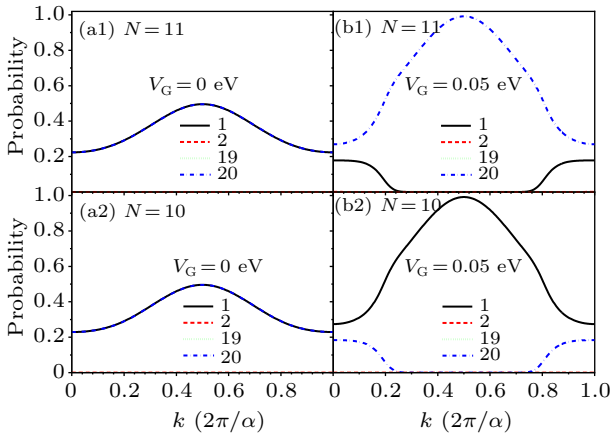


Fig. 5. (color online) The spacial probability at the edge sites 1, 2, 19, and 20 of edge states in two edge bands ($N = 10, 11$) without /with the I type of applied electric field shown in panels (a)/(b), respectively.

For two edge bands there are two special k points Γ ($k = 0$) and $k = 0.5$. Not considering electric field the band gap Δ_1 at Γ decreases with the increase of width shown in Fig. 3(a). When applying electric field, the degenerate two bands at $k = 0.5$ splits and open one another band gap Δ_2 shown in Fig. 6(a). For $N_w = 20$ the two band gaps Δ_1 and Δ_2 change with the applied electric potential, respectively, shown in Fig. 6(b). Obviously, for I, II, and IV types, the band gap Δ_2 at $k = 0.5$ *versus* the gate voltage is the same. It increases rapidly from zero and is over the band gap Δ_1. The band gap Δ_1 at Γ *versus* voltage is different for different types of electric field, respectively. For the band gap Δ_1 among four types of electric field it increases slowly in the type I. On the contrary, for the type II it increases fast and approaches to the Δ_2. From Fig. 6(b) for the types II and IV they have the same characteristic that the band gap Δ_1 is similar to the Δ_2 compared to other types. Comparing these two types the difference in them is the degree of opened gap when large electric field, the opened gap in the type II is three times larger than that in the type IV. Therefore, these results show that the band gap Δ_1 and Δ_2 is not only sensitive to the strength electric field, but also sensitive to the configuration of electric field distribution, especially for the Δ_2. We can expect that the linear optical absorption in the low-energy-excited region is different due to the different band gaps under the four types of electric field distribution configuration in the following paragraphs.

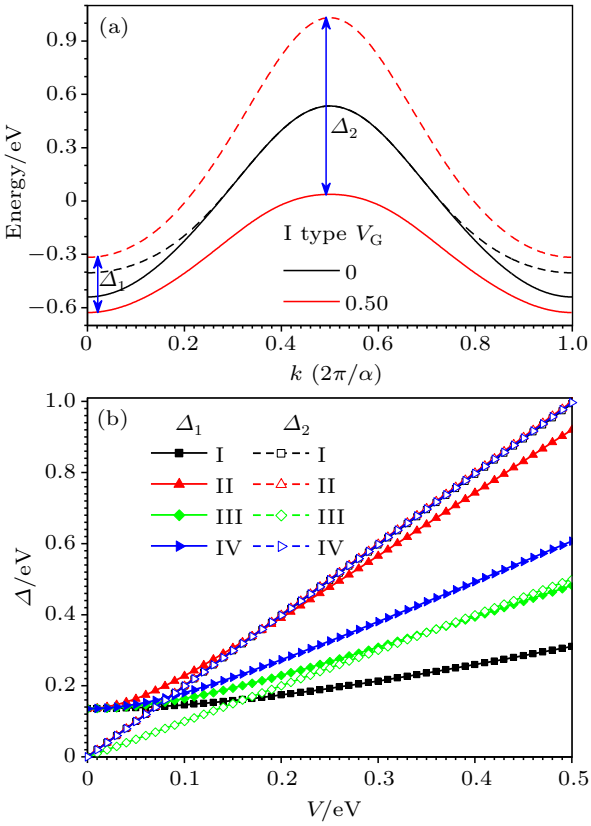


Fig. 6. (color online) The edge band structure without/with electric field in panel (a). (b) The two band gaps Δ_1 and Δ_2 at Γ point and $k = 0.5$ point change with the strength of electric field for four types of distribution configurations, respectively.

Subsequently, when the strength of electric field is taken as 0.5 eV, the band structures and the calculated linear optical absorption spectra for five types of electric field configuration are shown in Fig. 7 and Fig. 8, respectively. From the band structures in Fig. 7 we can find that the configuration of electric field tunes mainly the structure of two edge bands. The top of the band 11 is independent on the configuration of electric field. But the dip of the band 11 and the top and dip of the band 10 change with the configuration of electric field. For the fifth type of electric field configuration, the band gap Δ_1 decreases and the structure is the same to that for the third type. However, when $V_{GC} = 0.50$ eV the two edge bands is the same to that for the type II. Therefore, we can control the value of V_{GC} to tune the electric field configuration from one to another one. We consider four low-energy transitions at the Γ point among

four bands near the Fermi energy. Analyzing the dipole matrix elements between the four bands near the Fermi energy, we find that at $k = 0.5$ the y-component of dipole matrix element always is zero, although the band gap Δ_2 changes with the strength of electric filed. That is to say, the transition between two pure edge states in the two edge bands 10 and 11 at $k = 0.5$ is forbidden even if applying the electric field.

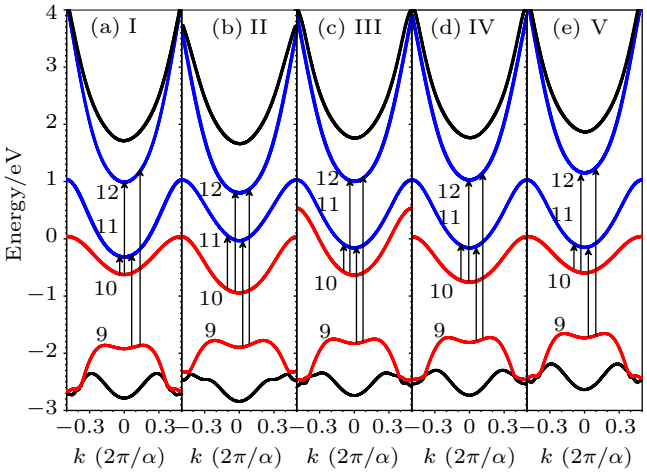


Fig. 7. (color online) The band structures of nZZ-BPNR with $N_w = 20$ under five types of electric field configuration. Here the strengths of gate voltages on different regions are $V_{GA} = 0.50$ eV, $V_{GB} = -0.50$ eV, and $V_{GC} = 0.50$ eV in panel (e) for the fifth type. The black vertical arrows denote the four low-energy transitions at the Γ point.

According to the band structure of two edge bands above obtained in Fig. 7, obviously, several low-energy-excited peaks appear in the region between 0 and 2.2 eV for x- (y)-polarized linear absorption spectra in Figs. 8(a) and 8(b). Compared with the data at $V = 0.50$ eV in Fig. 6(b), we find that the lowest-energy-excited peak called E_{11} in Figs. 8(a) and 8(b) originates from the band gap Δ_1 at Γ for five types (I–V) of electric field configuration, respectively. From Figs. 6(a) and 6(b) the position of the lowest-energy-excited peak can be tuned by the strength and the configurations of electric filed. Especially, the lowest-energy- excited peak for y-polarized incident light is much stronger than that for x-polarized light. For the type V using the strength of another gate voltage V_{GC} in the third region we can tune the band gap Δ_1, that is to say, the position of the lowest- energy-excited peak from the high energy to the lower one. At the same time, then band gap Δ_2 nearly does not change with the strength V_{GC}.

From Fig. 8(b) other low-energy-excited peaks appear near 1.7 eV corresponding to the transitions between 9 (10) and 11 (12), so called E_{12} (E_{21}). But the analysis of dipole matrix element shows that the transition E_{12} (E_{21}) are forbidden without the applied electric field. However, when applying electric field the forbidden is broken. Further, the E_{12} (E_{21}) peaks are mainly excited at the Γ point, not at $k = 0.5$ point. The splitting of the E_{12} peak and the E_{21} peak is dependent on the electric field configuration.

Compared with the spectra for various electric field configuration in Fig. 8(b), with the same strength of electric field the E_{11} peak for the second type configuration moves to the higher energy position 0.9 eV than other types. According to the data in Fig. 6(b) the energy position of E_{11} peak for the second type is the highest at all strength of electric field. For the first type configuration the E_{11} peak is at the lowest energy.

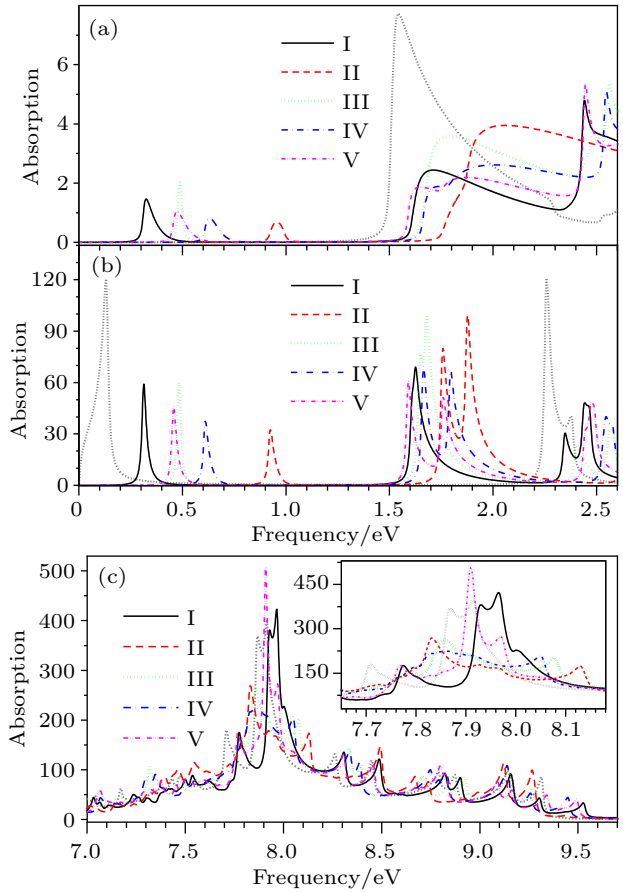


Fig. 8. (color online) For x- (y- and z)-polarized incident light the linear absorption spectra in panels (a), (b), and (c), respectively, under the five types of electric field with the strength ($V_{GA} = 0.5$ eV, $V_{GB} = -0.5$ eV, and $V_{GC} = 0.5$ eV). The gray dotted line is the spectrum without electric field for comparison.

4. Conclusion

In the summary, the obtained results show that the applied electric field not only open another band gap at $k = 0.5$ point, which is corresponding to the pure edge state, but also can change completely the special probabilities of edge states in the two edge bands. The strength of electric field can tune the two band gaps at the Γ point and 0.5 point. However, the transition at 0.5 point between two edge bands is forbidden. The lowest-excited-energy linear absorption peak E_{11} originates from the transition between two edge bands at the Γ point. Further, the second type of electric field configuration can move this lowest-excited-energy peak blue-shift larger than other configurations. Finally, one remarkable feature is that the second lowest-excited-energy forbidden peak

E_{12} and E_{21} are allowed by applying the electric field.

References

[1] Castellanos-Gomez A 2015 *J. Phys. Chem. Lett.* **6** 4280
[2] Rudenko A N, Yuan Shengjun and Katsnelson M I 2015 *Phys. Rev. B* **92** 085419
[3] Saroka V A, Lukyanchuk I, Portnoi M E and Abdelsalam H 2017 *Phys. Rev. B* **96** 085436
[4] Sousa J S de, Lino M A, Costa D R da, Chaves A, Pereira J M Jr and Farias G A 2017 *Phys. Rev. B* **96** 035122
[5] Debnath P C, Park K and Song Yong-Won 2018 *Small* **2** 1700315
[6] DhanabalanS C, Ponraj J S, Guo Z, Li S, Bao Q and Zhang H 2017 *Adv. Sci.* **4** 1600305
[7] Chandra Chowdhury and Ayan Datta 2017 *J. Phys. Chem. Lett.* **8** 2909
[8] Ma J, Lu S, Guo Z, Xu X, Zhang H, Tang D and Fan D 2015 *Opt. Express* **23** 22643
[9] Li J, Luo H, Zhai B, Lu R, Guo Z, Zhang H and Liu Y 2016 *Sci. Rep.* **6** 30361
[10] Guo Z, Chen S, Wang Z, Yang Z, Liu F, Xu Y, Wang J, Yi Y, Zhang H, Liao L, Chu P K and Yu X 2017 *Adv. Mater.* **29** 170381
[11] Yu L, Zhu Z, Gao A, Wang J, Miao F, Shi Y and Wang X 2018 *Nanotechnology* **29** 484001
[12] Li L L, Moldovan D, Xu W and Peeters F M 2017 *Nanotechnology* **28** 085702
[13] Sajadi E, Palomaki T, Fei Z, Zhao W, Bement P, Olsen C, LuescherS, Xu X, Folk J A and Cobden D H 2018 *Science* aar4426
[14] Fatemi V, Wu S, Cao Y, Bretheau L, Glbson Q D, Watanabe K, Taniguchi T, Cava R J and Jarillo-Herrero P 2018 *Science* aar4642
[15] Tran V and Yang L 2014 *Phys. Rev. B* **89** 245407
[16] Nourbakhsh Z and Asgari R 2016 *Phys. Rev. B* **94** 035437
[17] Ezawa M 2014 *New J. Phys.* **16** 115004
[18] Guo H, Lu N, Dai J, Wu X and Zeng X C 2014 *J. Phys. Chem. C* **118** 14051
[19] Maity A, Singh A and Sen P 2014 arXiv: 1404.2469
[20] Carvalho A, Rodin A S and Castro Neto A H 2014 arXiv: 1404.5115
[21] Peng X, Wei Q and Copple A 2014 *J. Appl. Phys.* **116** 144301)
[22] Sisakht E T, Zare M H and Fazileh F 2015 *Phys. Rev. B* **91** 085409
[23] Grujić M M, Ezawa M, Tadić M Ž and Peeters F M 2016 *Phys. Rev. B* **93** 245413
[24] Castro Neto A H, Guinea F, Peres N M R, Novoselov K S and Geim A K 2009 *Rev. Mod. Phys.* **81** 109
[25] Katsnelson M I 2012 *Graphene: Carbon in Two Dimensions* (Cambridge: Cambridge University Press)
[26] Fujita M, Wakabayashi K, Nakada K and Kusakabe K 1996 *J. Phys. Soc. Jpn* **65** 1920
[27] Son Y W, Cohen M L and Louie S G 2006 *Nature* **444** 347
[28] Ezawa M 2006 *Phys. Rev. B* **73** 045432
[29] Chaves A, Low T, Avouris P, Çakır D and Peeters F M 2015 *Phys. Rev. B* **91** 155311
[30] Pedersen T G 2017 *Phys. Rev. B* **95** 235419
[31] Hipolito F and Pedersen T G 2018 *Phys. Rev. B* **97** 035431
[32] Motavas S, Ivanov A and Nojeh A 2010 *Phys. Rev. B* **82** 085442
[33] Lin M F 2000 *Phys. Rev. B* **62** 13153
[34] Liu H, Schumacher S and Meier T 2013 *Phys. Rev. B* **88** 035429
[35] Liu H, Schumacher S and Meier T 2014 *Phys. Rev. B* **89** 155407
[36] Haug H and Koch S W 2009 *Quantum Theory of the Optical and Electronic Properties of Semiconductors*, 5th edn. (Singapore: World Scientific)
[37] Zaric S, Ostojic G N, Kono J, Shaver J, Moore V C and Strano M S 2004 *Science* **304** 1129
[38] Ehlen N, Senkovskiy B V, Fedorov A V, Perucchi A, Pietro P Di, Sanna A, Profeta G, Petaccia L and Gruneis A 2016 *Phys. Rev. B* **94** 245410
[39] Brown A and Rundqvist S 1965 *Acta Crystallogr.* **19** 684
[40] Lynge T B and Pedersen T G 2003 *Phys. Rev. B* **67** 075206
[41] Wang X and Liu H 2011 *Acta Phy. Sin.* **60** 047102 (in Chinese)
[42] Hu B, Liu N and Liu H 2018 *Journal of Nanjing Normal University* **41** 42 (in Chinese)
[43] Liu N, Hu B, Wei H and Liu H 2018 *Acta Phy. Sin.* **67** 117301 (in Chinese)